



In vitro transdermal delivery of therapeutic antibodies using maltose microneedles

Guohua Li^a, Advait Badkar^b, Sandeep Nema^b, Chandra Sekhar Kolli^a, Ajay K. Banga^{a,*}

^a Department of Pharmaceutical Sciences, College of Pharmacy and Health Sciences, Mercer University, 3001 Mercer University Drive, Atlanta, GA 30341, USA

^b Pharmaceutical Sciences – Global Biologics (Pharmaceutical R&D), Pfizer Inc. 700 Chesterfield Parkway (W), Chesterfield, MO 63017, USA

ARTICLE INFO

Article history:

Received 10 July 2008

Received in revised form 1 October 2008

Accepted 3 October 2008

Available online 19 October 2008

Keywords:

Microneedles

Human IgG

Transdermal delivery

Monoclonal antibody

ABSTRACT

This paper investigates the microneedle-mediated *in vitro* transdermal delivery of human IgG as a model protein and demonstrates its applicability to deliver a monoclonal antibody. Microchannels created by the treatment of maltose microneedles in full thickness hairless rat skin were visualized using methylene blue staining. Cryostat sections were prepared and stained using hematoxylin and eosin to locate the depth of penetration. *In vitro* penetration studies were conducted using freshly excised full thickness hairless rat skin and various parameters like needle length, number of needles and effect of donor concentration were examined. Pathway of IgG transport across skin was confirmed by immunohistochemical (IHC) studies. A monoclonal antibody was delivered under optimized conditions. Methylene blue was taken up by microchannels indicating disruption of the stratum corneum and cryosections showed that microneedles just reached the dermis. Human IgG delivery increased with increase in arrays of microneedles, concentration and length of microneedles. IHC studies demonstrated that IgG follows microchannels for transport across the skin. Transdermal delivery was also demonstrated for the monoclonal antibody. In conclusion, maltose microneedles provide a means for the transdermal delivery of macromolecules.

© 2008 Elsevier B.V. All rights reserved.

1. Introduction

Oral administration of proteins is therapeutically desirable but unlike conventional drug molecules, oral administration of proteins encounters significant proteolytic degradation and absorption barriers. Currently, proteins are mostly administered by parenteral administration but non-invasive routes of administration are desirable. One approach that has been investigated is the delivery via skin (McAllister et al., 2003; Meidan and Michniak, 2004; Schuetz et al., 2005; Levin et al., 2005; Coulman et al., 2006b). Proteins, being hydrophilic macromolecules, do not passively permeate across the skin; some enhancement strategies are needed to enable protein delivery into and across the skin. One such enhancement strategy is iontophoresis but delivery may be limited to proteins with a maximum molecular weight of 10–15 kDa (Banga, 2006b). For larger molecules, one possible minimally invasive approach is the physical disruption of stratum corneum by a variety of means such as radiofrequency ablation (Birchall et al., 2006), thermal microporation (Badkar et al., 2007), or usage of microneedles (Coulman et al., 2006a; Banga, 2006a).

Application of microneedles for transdermal delivery was first reported in 1998 (Henry et al., 1998). Since then, there has been an increasing interest in this field for pharmaceutical applications. Transdermal delivery of insulin *in vivo* was studied using solid microneedles, and it was demonstrated that microneedles increased insulin delivery and thereby decreased blood glucose levels in diabetic hairless rats (Martanto et al., 2004). Microneedles were combined with iontophoresis for transdermal delivery of an oligonucleotide *in vivo* and authors demonstrated that the combined approach increased transdermal flux by 100-fold relative to iontophoresis used alone (Lin et al., 2001). Another approach that has been investigated more widely is an integrated delivery system comprising of a hypodermic needle and a transdermal patch (Coulman et al., 2006a).

Microneedles, typically made of silicon, metal and polymer, can penetrate the skin to create micron-sized pores that are big enough to permit the transport of macromolecules and even microparticles (Prausnitz, 2004). Microneedles are usually designed to penetrate down to the dermal layer of skin, but not to reach and stimulate the dermal nerves. Safety studies performed with microneedles ranging in length between 500 and 1500 μm showed that pain induced by the microneedles is significantly lower when compared to hypodermic needles (Gill, 2006).

A purified human immunoglobulin, IgG, with a MW of about 150 kDa was employed as the model drug for macromolecules.

* Corresponding author. Tel.: +1 678 547 6243; fax: +1 678 547 6423.
E-mail address: banga.ak@mercer.edu (A.K. Banga).

This is the first report on the delivery of a 150-kDa macromolecule using soluble microneedles through the skin. Initial studies were conducted with human IgG and once factors affecting delivery were optimized, a monoclonal antibody was further studied for the applicability of microneedles for delivering other macromolecules. Studies were done using freshly excised skin. Other researchers have also used an excised skin model for microneedle-mediated delivery (Amnon et al., 2003; Verbaan et al., 2007; Xie et al., 2005). We have demonstrated *in vivo* (data not shown) by methylene blue staining and TEWL measurements that micropores stay open for at least 24 h when occluded with a formulation.

2. Materials and methods

2.1. Materials

Microneedles were developed and supplied by Texmac Inc. (USA). Purified human IgG, goat serum, avidin and biotin were purchased from Sigma (St. Louis, MO, USA). Monoclonal antibody of IgG was provided by Pfizer Inc. (Chesterfield, MO, USA). Biotinylated anti-human IgG (H+L), vector aqueous anti-fade fluorescent mounting medium, and FITC-Avidin D were purchased from Vector Labs (Burlingame, CA, USA). Hematoxylin, eosin, phosphate buffered saline and polysine microscope slides were purchased from Fisher Scientific (Pittsburgh, PA, USA).

Hairless rats were obtained from Charles River (Wilmington, MA, USA) and were housed in the animal facility at Mercer University until used. Study was approved by the Mercer University IACUC Committee.

2.2. Methods

2.2.1. Visualization of microneedles and microchannels

To facilitate imaging studies, skin treated with 500 μm long microneedles was stained with methylene blue for 2 min. It was rinsed quickly with PBS (pH 7.4), and excessive stain was removed using alcohol swabs (Birchall et al., 2006). Pictures of microneedles before treatment and pictures of the stained skin following pretreatment were collected using a digital camera (Canon, USA) or a video microscope (Hi-Scope KH2200, Hirox Co., Japan). A control was employed to demonstrate that the skin disruption is due to the microneedles alone and not due to pressure resulting from the insertion procedure. For this, an empty microneedle base with all the needles removed was pressed onto the skin with the same pressure as with the microneedles. Microneedles were also examined using field emission scanning electron microscope (Hitachi, S4100, Japan) integrated with a critical dimension measurement system. Primary beam accelerating voltage was 15 kV and secondary ion images were collected.

2.2.2. Histology of micro-conduits within skin

Freshly excised full thickness hairless rat skin treated with 500 μm long microneedles was stained with methylene blue for 2 min, rinsed in PBS to wash off the dye and excess dye was further cleaned using alcohol swabs. The skin tissue was subsequently embedded in OCT medium snap frozen in liquid nitrogen and stored overnight at -80°C . The cryosectioning of frozen tissue was performed using a cryomicrotome (Histostat Cryostat Microtome, Buffalo, NY) to produce skin sections with thickness measuring between 8 and 12 μm . These were then stained with hematoxylin and eosin (H&E), and the images were examined using a microscope.

2.2.3. *In vitro* studies

Microneedles (500 or 200 μm long) were used for the *in vitro* studies. They were stacked in layers to obtain the desired microneedle density. Single layer of 500 μm long microneedles contained 27 needles per layer and can be stacked in two or three parallel layers to give 54 and 81 microneedles per assembly, respectively. A single layer of 200 μm long microneedles contained 48 microneedles per layer.

Full thickness skin, freshly excised from hairless rats was manually inserted with maltose microneedles using a force of about 250 g monitored on a weight balance. Once the needles were inserted into skin, the cardboard base of microneedles was then held straight in position for 1 min to allow the microneedles to dissolve in the skin. Following insertion, the cardboard was observed under a stereomicroscope (LEICA MZ6, 6.3–40 \times) to make sure all the needles were inserted into the skin. The maltose microneedles dissolved immediately but the channels remained open for at least 24 h when covered with a drug solution (unpublished data). Treated skin was then mounted on static type Franz diffusion cells having a diffusion area of 0.64 cm^2 (PermeGear, Bethlehem, PA). Donor solution was composed of human IgG solution (1–40 mg/ml in phosphate buffer pH 7.4) and the receptor compartments contained 5 ml phosphate buffer (pH 7.4). Receptor cells were maintained at 37°C under stirring. Influence of various parameters like the number of microneedles (single layer with 27 needles or two layers with 54 needles), length of the microneedles (200 and 500 μm) and donor concentration (1, 5, 20, and 40 mg/ml) on the transdermal delivery of human IgG was investigated. Skin treated with just the cardboard base of the microneedle holder without microneedles served as pressure control for the experiments. All the studies were performed using purified human IgG except for one study in which human monoclonal antibody was used.

Aliquots of 500 μl were collected at various time intervals from the receptor and immediately replenished with the same volume of receptor solution. The samples were stored in a refrigerator until they were analyzed. The amount of IgG diffused was determined by quantifying the samples using ELISA. All the *in vitro* studies were performed in triplicate unless otherwise mentioned and results were presented as mean \pm S.E.

2.2.4. Quantitative analysis

Samples were analyzed using sandwich ELISA (Human IgG ELISA quantitation kit, Bethyl Laboratories, Inc., Montgomery, TX, USA). Briefly, 96-well plates (Nunc-Immuno Module, Nalge Nunc International, Kaysville, UT, USA) were coated with 100 μl /well of goat anti-human IgG antibody (10 $\mu\text{g}/\text{ml}$ in coating buffer) and incubated at room temperature for 1 h. The plates were washed three times with wash solution (50 mM Tris containing 0.14 M NaCl and 0.05% Tween 20, pH 8.0) and then blocked using blocking solution (50 mM Tris containing 0.14 M NaCl and 1% BSA, pH 8.0). The plates were washed again three more times and incubated with 100 μl of test sample for 1 h (samples were diluted appropriately when needed) followed by five subsequent washings. HRP-conjugated antibody (100 μl) was then added and incubated for 1 h at room temperature. Later, 100 μl of substrate (TMB, Sigma) was added and further incubated for 5–30 min, and the reaction was terminated by the addition of 2 M H_2SO_4 . Absorbance was measured at 450 nm using an ELx 800 UV microtiter plate reader (Bio-Tek Instruments, Winooski VT, USA).

2.2.5. Extraction of IgG from skin

Amount of drug retained in the skin following *in vitro* study provides an indirect evidence of amount permeated through the skin during the study. The skin pieces ($n=3$) were collected after the completion of the *in vitro* study. The area of the skin exposed to the

drug was isolated and washed three times, each for 20 min with PBS (pH 7.4). The skin portion was then tape stripped twice using Transpore tape (3M, St. Paul, MN, USA) to remove the surface bound IgG; cut into small pieces and transferred into a vial containing 0.5 ml of PBS buffer and homogenized over ice using a homogenizer (OMNI International, Marietta, GA, USA). The resulting suspension was centrifuged at 10,000 rpm for 10 min while maintaining a temperature of 4 °C and the supernatant was analyzed by ELISA as mentioned in the earlier section.

Extraction efficiency of human IgG from skin was determined by superficially injecting 50 μ l of human IgG (0.5, 1.0, and 2.0 μ g/ml) into skin pieces ($n=3$ for each concentration) and allowing to stand for 3 h at room temperature. Following equilibration, skin pieces were homogenized over ice in PBS buffer (pH 7.4) and centrifuged at 4 °C at 10,000 rpm for 10 min. Samples were then analyzed by ELISA and recovery was calculated to be $73.6 \pm 4.1\%$.

2.2.6. Immunohistochemical studies

Hairless rat skin collected following the *in vitro* study was frozen and sections were prepared for IHC studies. Before staining, frozen sections were thawed to room temperature and fixed over ice-cold acetone for 5 min and later air dried for 30 min. Skin sections were then rinsed twice with washing buffer (PBS pH 7.2 containing 0.05% Tween 20) for 2 min each and later normal serum blocking was performed. Since this study involved avidin–biotin system, avidin/biotin blocking was performed after normal serum block. Sections were washed thrice in washing buffer for 2 min each and then incubated in biotinylated anti-human IgG solution (1:500 in PBS with pH 7.2) for 1 h at room temperature. They were rinsed thrice in buffer for 2 min each and were then incubated in FITC-Avidin D in PBS (pH 7.2) solution for 1 h at room temperature while protecting slides from light. It was again rinsed thrice in washing buffer for 2 min each, mounted with vector aqueous anti-fade fluorescent mounting medium and slides were examined using a fluorescent microscope (Leitz Fluovert Wetzlar, Germany, 25 \times).

3. Results

3.1. Visualization of microneedles and microchannels

Fig. 1(a) is a video microscopic picture of single layer maltose microneedles and a further magnified image of individual microneedles was obtained by scanning electron microscopy and presented in Fig. 1(b). These pictures show intact needles spaced uniformly along the cardboard base.

Microchannels created in the skin can be visualized through their ability to uptake methylene blue marker (Birchall et al., 2006). Fig. 1(c) is a picture of full thickness hairless rat skin stained with methylene blue following treatment with six-layered microneedles. Areas of the skin breached by microneedles took up the dye. There was no evidence of any damage caused by the base of the microneedles. All the layers and almost all of the microneedles penetrated the skin as seen in Fig. 1(c).

Fig. 2(a–c) shows cryosections of skin pretreated with microneedles. The skin portions around the microchannel maintained normal structure with intact stratum corneum [Fig. 2(a)] whereas the microchannel [Fig. 2(b and c)] was seen as deep indentation with disrupted stratum corneum at the base, extending through the epidermis and just up to superficial dermal layer. Also, localization of blue tissue could be observed at the base of microchannels. Fig. 2(d) is the SEM image (primary accelerating voltage used was 10 kV) of the cryosection where the microchannel

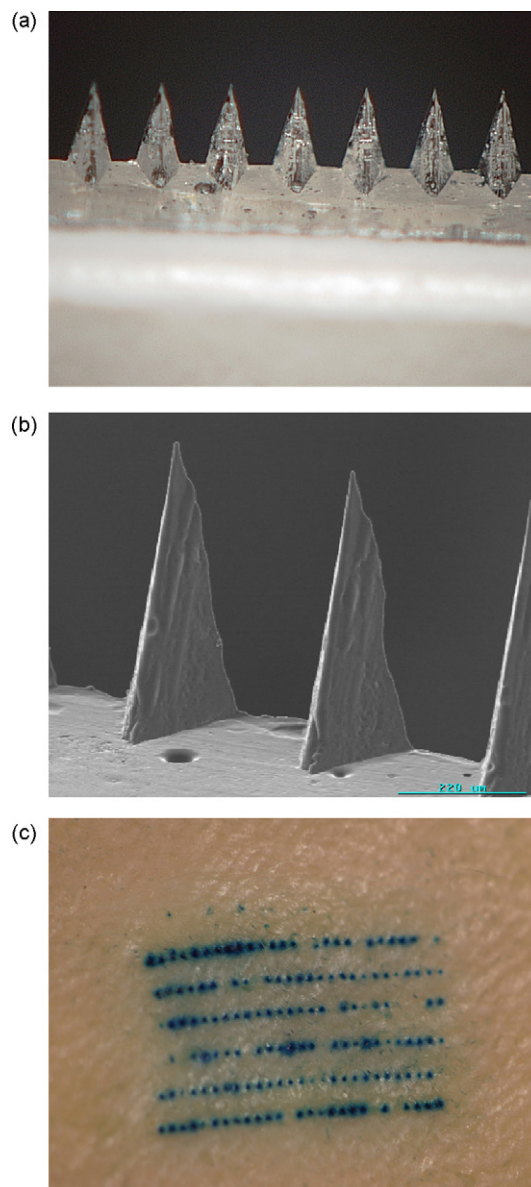


Fig. 1. (a) Single layer microneedles as seen by a video microscope. (b) SEM image of a portion of single maltose microneedle layer with needle length of 500 μ m. (c) Photomicrograph of methylene blue-stained skin treated with six layers of microneedles stacked in parallel.

can be clearly visualized here as an indentation along the normal skin.

3.2. Effect of microneedle layers

The microneedles employed in these studies have 27 needles per layer and were stacked in parallel layers to result in desired pore density. The effect of increasing number of layers and thereby pores on the delivery of IgG (500 μ l, 20 mg/ml) is shown in Fig. 3. Following pretreatment, the steady state flux increased from 66.7 with single layer to 660 ng/(cm² h) with two layers of 500 μ m long microneedles.

3.3. Effect of drug concentration

The influence of drug concentration on transdermal delivery was also determined (Fig. 4). In this specific study, skin was pre-

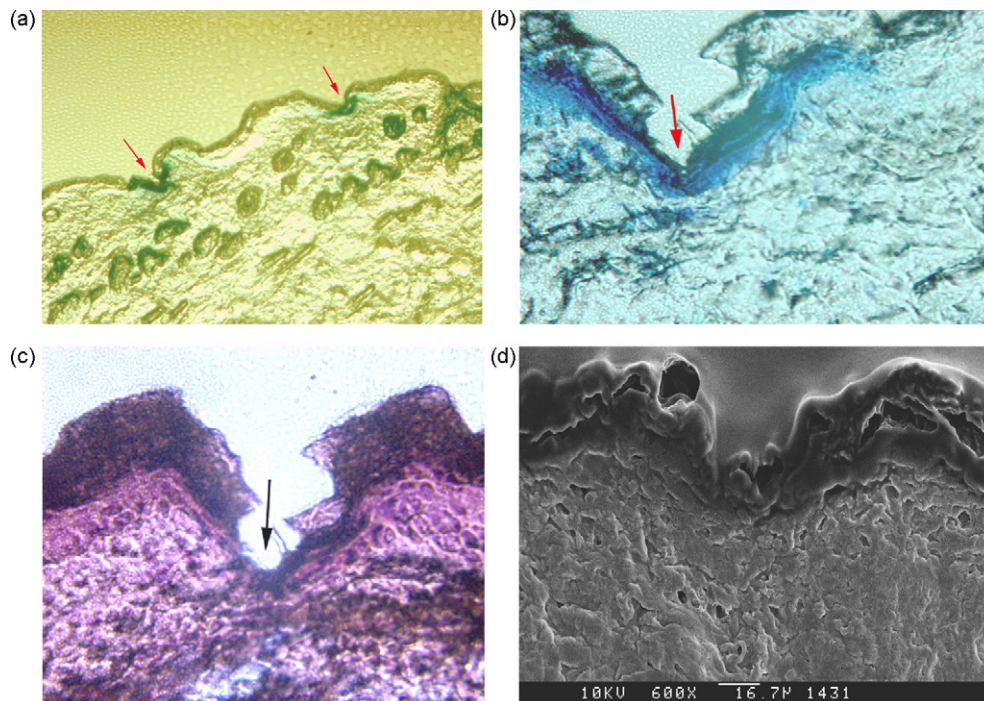


Fig. 2. (a) Histology of unstained cryosection of microneedle treated rat skin, in magnified view. (b) H&E-stained cryosection following pretreatment. (c) Blue at the bottom of pore indicates the methylene blue staining. (d) SEM image of skin section following treatment with microneedles.

treated with two-layered maltose microneedles and 200 μ l IgG (1, 5, 20 or 40 mg/ml) was applied to each donor. Increasing IgG transport with increased concentration of drug in donor was observed up to 20 mg/ml concentration. A maximum flux of 179 $\text{ng}/(\text{cm}^2 \text{ h})$ was achieved for the 20 mg/ml concentration. Though the mean cumulative amount and steady state flux with 40 mg/ml as donor were less than that of 20 mg/ml, the difference was found to be not statistically significant ($P < 0.05$).

3.4. Effect of microneedle length

The influence of microneedle length on IgG delivery was investigated (Fig. 5). Single-layer microneedles with 200 or 500 μm in length were inserted twice on each skin piece and a 500- μl of 20 mg/ml IgG was used as donor solution. The results show that length of needles has an effect on the delivery. Briefly, when the length of needle was increased from 200 to 500 μm , steady state flux changed from 27.07 to 102.09 $\text{ng}/(\text{cm}^2 \text{ h})$.

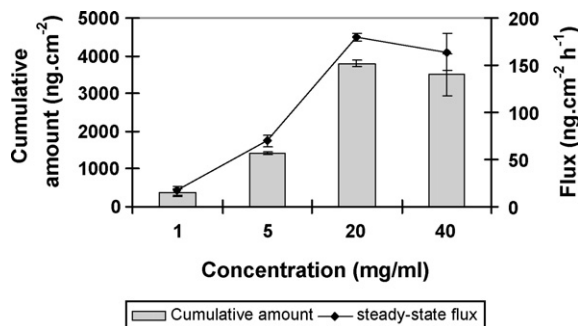


Fig. 4. Cumulative amounts of human IgG permeated and steady state flux across hairless rat skin pretreated with two-layered microneedles (54 needles, 500 μm long) during 24 h of transdermal delivery with 200 μl of donor at 40, 20, 5 or 1 mg/ml of human IgG concentrations (mean \pm S.E.) ($n = 3$).

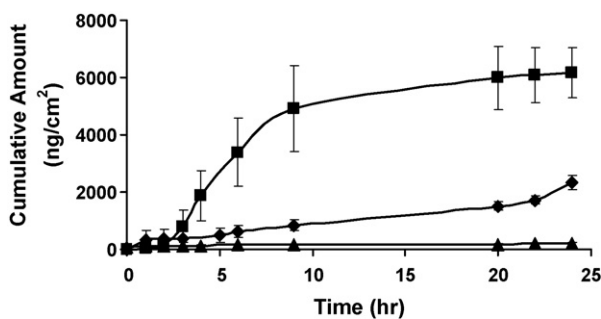


Fig. 3. The *in vitro* permeation profile of human IgG (500 μl , 20 mg/ml) across skin following treatment with single layer (◆, 27 needles, 500 μm long) or two layers (■, 54 needles, 500 μm long) of maltose microneedles and cardboard base without microneedles serving as pressure control (▲) (mean \pm S.E.) ($n = 3$).

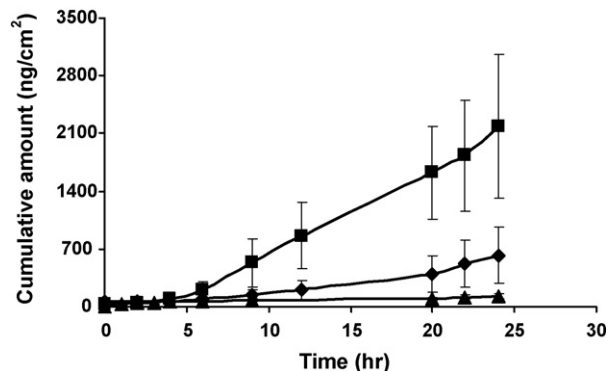


Fig. 5. The effect of microneedle arrays having different lengths/numbers of microneedles on IgG permeation *in vitro*: microneedles with 500 μm long MN (■, single layer with 27 needles, insertion twice) and 200 μm long MN (◆, single layer with 48 needles, insertion twice) were compared to control (▲). hIgG was 500 μl of 20 mg/ml in donor cell (mean \pm S.E.) ($n = 3$).

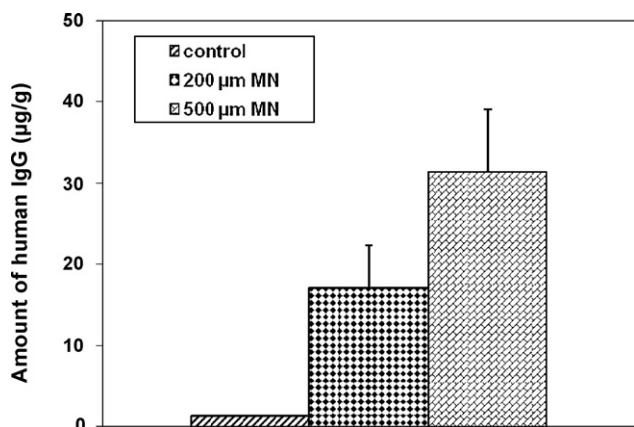


Fig. 6. Extraction of human IgG from exposed area following *in vitro* study across hairless rat skin treated with microneedles following passive delivery.

3.5. Extraction of IgG from skin

Skin extractions were carried out following *in vitro* study to estimate the amount of IgG retained in the skin (Fig. 6). Results show that skin retention of IgG was high ($31.4 \pm 7.6 \mu\text{g/g}$) when skin was treated with $500 \mu\text{m}$ long microneedles as compared to similar treatment but with $200 \mu\text{m}$ long microneedles ($17.0 \pm 5.3 \mu\text{g/g}$).

3.6. Immunohistochemistry

Fig. 7(a and b) shows fluorescent micrographs of IgG permeation pathways in hairless rat skin pretreated with microneedles. Fig. 7(a) indicates that IgG is transported down through the microchannel and Fig. 7(b) shows IgG diffused out radically into the surrounding epidermal tissue. Dark areas without any fluorescence indicate absence of IgG.

3.7. *In vitro* transdermal delivery of monoclonal antibody

In all the previously mentioned studies, purified human IgG was used as a model drug for large proteins in transdermal delivery, and later the feasibility of microneedle-mediated transdermal delivery was further investigated using a human monoclonal antibody IgG to demonstrate the applicability of this technique for delivery of macromolecules. Fig. 8 represents the penetration profile of the monoclonal antibody through hairless rat skin treated with three single layer needles (81 pores in total). Significant enhancement in transdermal delivery following pretreatment with microneedles as compared to passive was observed. The

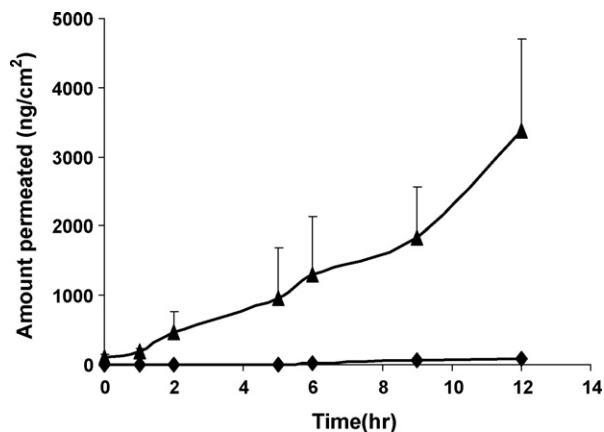


Fig. 8. *In vitro* transdermal delivery of the model monoclonal antibody ($500 \mu\text{l}$ of 5 mg/ml) after skin was treated with single line microneedles inserted three times (81 needles in total) (▲), and treatment with base without microneedles that serves as pressure control (◆) (mean \pm S.E.) ($n=3$).

steady state flux was $269.5 \text{ ng}/(\text{cm}^2 \text{ h})$ following microneedles pretreatment.

4. Discussion

Delivery of purified human IgG and a monoclonal antibody *in vitro* across hairless rat skin was investigated and direct visualization of IgG in the microchannels was possible with immunohistochemical studies. Ability of the microneedles to create the microchannels in the skin was confirmed from methylene blue staining which could stain the microchannels created by microneedles. Intact skin with hydrophobic stratum corneum cannot take up the hydrophilic low molecular weight methylene blue but once the skin is breached due to pretreatment with microneedles, integrity of stratum corneum is lost and methylene blue diffuses through the newly created microchannels in the skin.

The maltose microneedles had tips that were sharp enough ($3 \mu\text{m}$) to pierce the stratum corneum for creating microchannels. Davis et al. measured and predicted the insertion force and fracture force of microneedles, results showed that insertion forces of $10\text{--}300 \text{ g}$ were sufficiently low to permit insertion by hand (Davis et al., 2004). However, this insertion force is greatly dependent on the sharpness of the microneedle tip. In our study about 250 g of insertion force was sufficient enough for manual insertion of microneedles into the skin to ensure complete penetration.

The deep indentation observed (Fig. 2) was a result of applied pressure during the insertion of microneedles. Pressure applied

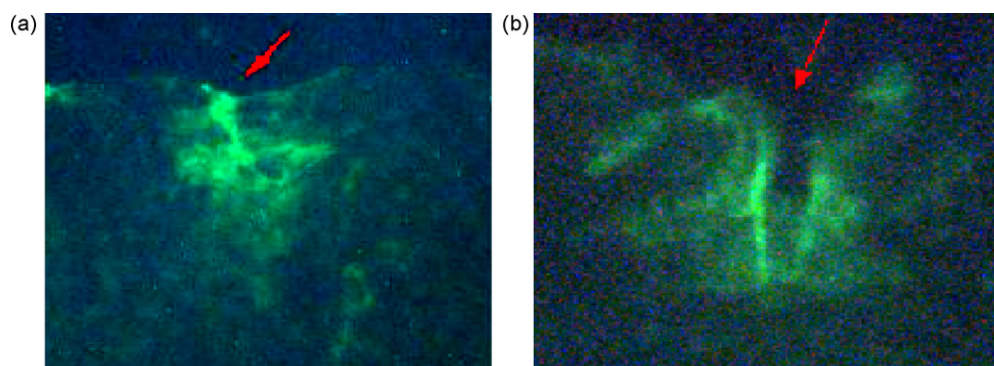


Fig. 7. IHC micrographs of permeation pathways for IgG in hairless rat skin, following treatment with $500 \mu\text{m}$ microneedles. IgG is transported down through the stratum corneum into the epidermal tissue via the microchannels exclusively (bright areas). Dark areas indicate lack of fluorescence.

first indents the skin because of the elastic nature of skin and after a sufficient pressure is applied, penetration of the needles into the skin occurs. This results in only a part of the microneedle penetrating through the stratum corneum and our observation regarding effective depth of penetration of microneedles was consistent with earlier reports in the literature (Martanto et al., 2006). The depth of penetration was just sufficient to reach the superficial dermal layer.

Increased delivery with increased number of microneedle layers shows the effectiveness of stacking microneedles in parallel to increase the number of pores per unit area. Control experiments conducted (Figs. 3 and 8) indicate that IgG did not permeate through skin just because of pressure applied by the microneedle holder but the delivery was due to the microneedles causing microscopic channels for transport. This offers an additional parameter in addition to drug concentration and patch size for optimizing the drug delivery.

Enhanced transdermal IgG transport was observed with increase in donor concentration up to a particular concentration following pretreatment with microneedles. Assuming 250 microneedles per cm² of skin and a linear extrapolation of flux, a flux of about 12 ng/(h pore) can be extrapolated to a delivery of 0.72 mg over 24 h using a 10 cm² patch. This flux could be sufficient for potential dermatological indications of monoclonal antibodies. More importantly, this shows feasibility of delivery of macromolecules across microporated skin. Further increase in flux should be possible with optimal formulation and device design. However, when the donor concentration was above 20 mg/ml, IgG delivery did not increase. This may be due to saturation of the boundary layer relative to the donor solution after which the transport becomes independent of concentration.

Microneedle arrays having different lengths/numbers of maltose microneedles affected transdermal delivery of IgG, with 500 μm long microneedles delivering more IgG across skin compared to 200 μm counterparts. This was consistent with reports by Widera et al. who investigated the influence of needles with lengths of 225, 400 and 600 μm on delivery of ovalbumin *in vivo*, and demonstrated that the needle length has an effect on delivery into the skin (Widera et al., 2006). However, since the number of microneedles in the array also changes as the length changes, this is not a clear comparison. In this study, though 200 μm long microneedles have 48 microneedles in a layer, it is possible that most of them might not have pierced the skin or at least not pierced to a depth sufficient to increase the transport of molecules. These shorter needles were observed to be less sturdy mechanically which may also be a contributing factor. The lower delivery was also confirmed from the skin extraction data (Fig. 6) that shows increased skin localization of IgG with 500 μm long microneedles as compared to 200 μm.

IHC has been used by researchers to demonstrate the localization of growth hormone-binding protein in rats (Lobie et al., 1992) and this technique has also been used to determine the growth hormone receptor in squamous cell carcinoma of the skin (Stanimirovic et al., 2004). Our results demonstrate the applicability of IHC to visualize the localization of human IgG around the microchannels. The transport of IgG appears to have taken place exclusively through microchannels created by microneedles (Fig. 7a and b). Fluorescence was observed primarily in the areas surrounding the microchannels. Fluorescence was not observed in the follicular shafts or the areas away from microchannels where the stratum corneum remained intact. Therefore, these studies support our earlier observations that transport of IgG across the skin takes place through microchannels created by microneedles.

The enhanced transdermal delivery was also demonstrated for the monoclonal antibody. It was shown that flux [269.53 ng/(cm² h)] of the monoclonal antibody enhanced sig-

nificantly following treatment with microneedles (Fig. 8). This enhancement was achieved by using monoclonal antibody with 5 mg/ml in PBS as donor. This demonstrates the ability of maltose microneedles to deliver large model molecules such as IgG and extends to the delivery of therapeutically relevant monoclonal antibodies.

5. Conclusions

Maltose microneedles that can dissolve in the skin upon insertion have been used for the percutaneous administration of therapeutic molecules. The microneedles were sufficiently strong to pierce the skin and when inserted into hairless rat skin, they penetrated the stratum corneum creating micro-scale conduits for percutaneous transport of macromolecules. Purified human IgG and a model monoclonal antibody were delivered *in vitro*. Localization of these molecules was seen just in and around the microchannels created by microneedles. Delivery of human IgG was influenced by various factors like number of microneedles, length of the microneedles and donor concentration.

Acknowledgements

We thank Pfizer for sponsoring this project and Ms. Yi-Ying Yu at Mercer University for proofreading the manuscript.

References

- Amnon, C.S., Krymberka, I., Danielb, D., Hannanb, T., Sohn, Z., Levin, G., 2003. Radiofrequency-driven skin microchanneling as a new way for electrically assisted transdermal delivery of hydrophilic drugs. *J. Control. Release* 89, 311–320.
- Badkar, A.V., Smith, A.M., Eppstein, J.A., Banga, A.K., 2007. Transdermal delivery of interferon alpha-2b using microporation and iontophoresis in hairless rats. *Pharm. Res.* 24, 1389–1395.
- Banga, A.K., 2006a. New technologies to allow transdermal delivery of therapeutic proteins and small water-soluble drugs. *Am. J. Drug Deliv.* 4, 221–230.
- Banga, A.K., 2006b. *Therapeutic Peptides and Proteins: Formulation Processing and Delivery Systems*, 2nd ed. Taylor and Francis.
- Birchall, J., Coulman, S., Anstey, A., Gateley, C., Sweetland, H., Gershonowitz, A., Neville, L., Levin, G., 2006. Cutaneous gene expression of plasmid DNA in excised human skin following delivery via microchannels created by radio frequency ablation. *Int. J. Pharm.* 312, 15–23.
- Coulman, S., Allender, C., Birchall, J., 2006a. Microneedles and other physical methods for overcoming the stratum corneum barrier for cutaneous gene therapy. *Crit. Rev. Ther. Drug Carrier Syst.* 23, 205–258.
- Coulman, S.A., Barrow, D., Anstey, A., Gateley, C., Morrissey, A., Wilke, N., Allender, C., Brain, K., Birchall, J.C., 2006b. Minimally invasive cutaneous delivery of macromolecules and plasmid DNA via microneedles. *Curr. Drug Deliv.* 3, 65–75.
- Davis, S.P., Landis, B.J., Adams, Z.H., Allen, M.G., Prausnitz, M.R., 2004. Insertion of microneedles into skin: measurement and prediction of insertion force and needle fracture force. *J. Biomech.* 37, 1155–1163.
- Gill, H.S., 2006. Effect of microneedle design on pain in human subjects. *Internet.* 11-16-2006.
- Henry, S., McAllister, D.V., Allen, M.G., Prausnitz, M.R., 1998. Microfabricated microneedles: a novel approach to transdermal drug delivery. *J. Pharm. Sci.* 87, 922–925.
- Levin, G., Gershonowitz, A., Sacks, H., Stern, M., Sherman, A., Rudaev, S., Zivin, I., Phillip, M., 2005. Transdermal delivery of human growth hormone through RF-microchannels. *Pharm. Res.* 22, 550–555.
- Lin, W., Cormier, M., Samiee, A., Griffin, A., Johnson, B., Teng, C.L., Hardee, G.E., Daddona, P.E., 2001. Transdermal delivery of antisense oligonucleotides with microprojection patch (Macroflux) technology. *Pharm. Res.* 18, 1789–1793.
- Lobie, P.E., Garcia-Aragon, J., Wang, B.S., Baumbach, W.R., Waters, M.J., 1992. Cellular localization of the growth hormone binding protein in the rat. *Endocrinology* 130, 3057–3065.
- Martanto, W., Davis, S.P., Holiday, N.R., Wang, J., Gill, H.S., Prausnitz, M.R., 2004. Transdermal delivery of insulin using microneedles *in vivo*. *Pharm. Res.* 21, 947–952.
- Martanto, W., Moore, J.S., Couse, T., Prausnitz, M.R., 2006. Mechanism of fluid infusion during microneedle insertion and retraction. *J. Control. Release* 112, 357–361.
- McAllister, D.V., Wang, P.M., Davis, S.P., Park, J.H., Canatella, P.J., Allen, M.G., Prausnitz, M.R., 2003. Microfabricated needles for transdermal delivery of macromolecules and nanoparticles: fabrication methods and transport studies. *Proc. Natl. Acad. Sci. U.S.A.* 100, 13755–13760.

- Meidan, V.M., Michniak, B.B., 2004. Emerging technologies in transdermal therapeutics. *Am. J. Ther.* 11, 312–316.
- Prausnitz, M.R., 2004. Microneedles for transdermal drug delivery. *Adv. Drug Deliv. Rev.* 56, 581–587.
- Schuetz, Y.B., Naik, A., Guy, R.H., Kalia, Y.N., 2005. Emerging strategies for the transdermal delivery of peptide and protein drugs. *Expert Opin. Drug Deliv.* 2, 533–548.
- Stanimirovic, A., Cupic, H., Tomas, D., Bosnjak, B., Balicevic, D., Kruslin, B., Belicza, M., 2004. Immunohistochemical determination of the growth hormone receptor in squamous cell carcinoma of the skin. *Acta Dermatoven APA* 13, 3–8.
- Verbaan, F.J., Bal, S.M., Van den Berg, D.J., Groenink, W.H.H., Verpoorten, H., Lutge, R., Bouwstra, J.A., 2007. Assembled microneedle arrays enhance the transport of compounds varying over a large range of molecular weight across human dermatomed skin. *J. Control. Release* 117, 238–245).
- Widera, G., Johnson, J., Kim, L., Libiran, L., Nyam, K., Daddona, P.E., Cormier, M., 2006. Effect of delivery parameters on immunization to ovalbumin following intracutaneous administration by a coated microneedle array patch system. *Vaccine* 24, 1653–1664.
- Xie, Y., Xu, B., Gao, Y., 2005. Controlled transdermal delivery of model drug compounds by MEMS microneedle array. *Nanomed.: Nanotechnol. Biol. Med.* 1, 184–190.